Physica 127B (1984) 257–263
North-Holland, Amsterdam

FIRST PRINCIPLE THEORY OF METALLIC MAGNETISM

J. KÜBLER
Institut für Festköperphysik, Technische Hochschule, D-6100 Darmstadt, Fed. Rep. Germany

Self-consistent spin-polarized energy-band calculations are used to explain the trends in the ferromagnetic moments of transition-metal alloys. It is demonstrated that a large amount of magnetization data become interpretable by using the generalized Slater-Pauling curve recently introduced by Williams et al. The discussion includes Heusler alloys of both $L2_1$ and $C1_b$ structure for which exchange constants and hence the Curie temperatures can be estimated theoretically. CoMnSb is treated in detail and is shown to belong to the class of half-metallic ferromagnets first discovered by de Groot et al. Also included will be Fe_3Cr and Au_4V which represent interesting examples of itinerant ferromagnetism.

1. Introduction

As is well known, the magnetic moments of a great number of ferromagnetic 3d metals and alloys can conveniently be arranged on the Slater–Pauling curve [1]. The systematics that results reveals some of the physics of how the moments are formed. But departures from regular behavior occur which obscure the general picture. Recently, the theories of Friedel [2], Terakura and Kanamori [3] were used by Williams et al. [4] to construct a generalization of the Slater–Pauling curve, called the Generalized Slater–Pauling curve (GSP). The underlying idea is remarkably simple. The magnetic moment per atom (in μ_B) is given by

$$M = N^{\uparrow} - N^{\downarrow}, \tag{1}$$

where $N^{\uparrow}(N^{\downarrow})$ is the number of majority (minority) spin electrons per atom. Neutrality requires

$$Z = N^{\uparrow} + N^{\downarrow}, \tag{2}$$

where Z is the number of valence electrons per atom. Eliminating either $N^{\downarrow}$ or $N^{\uparrow}$ from eqs. (1) and (2) one gets relations between the magnetization and the number of valence electrons which, on first sight, seem trivial, namely

$$M = 2N^{\uparrow} - Z, \tag{3}$$

or

$$M = Z - 2N^{\downarrow}. \tag{4}$$

For many transition metals and alloys (but not all), it is the number of *majority-spin* d electrons, $N_d^{\uparrow}$ that is the leading contribution to $N^{\uparrow}$. The crucial observation of Friedel [2] was that this number is exactly 0 or 5, depending on the case in question. Adding to this the observation that the remaining number of majority non-d electrons is small and easily estimated, Williams et al. [4] defined the concept of *magnetic valence*, Z_m,

$$Z_m = 2N_d^{\uparrow} - Z. \tag{5}$$

The right-hand side of eq. (3) is, therefore, Z_m plus a small correction and hence M is easily estimated. In section 2 we will deal with those metals and alloys for which the magnetic valence Z_m is the appropriate variable to describe the magnetic moment. Examples of this are Ni, Co, and alloys like NiCu, CoCr, FeNi, etc. But also more exotic systems like VAu_4 belong to this class as we will show.

There are, however, a number of interesting cases, where it is the right hand side of eq. (4) rather than eq. (3) which is easily estimated. Here the appropriate variable to describe the magnetic moment per atom is the average number of valence electrons, Z, and $N^{\downarrow}$ is very close to or exactly 3. We will deal with these cases in section 3 emphasizing particularly Heusler alloys with $C1_b$ structure. An important tool for the present study are band structure calculations. We will give details for VAu_4,

CoMnSb, and $CrFe_3$. In section 4, finally, we show that band structure techniques together with total-energy results allow estimates of the paramagnetic Curie temperatures for those systems where the magnetic moments are localized. Results are given for Heusler alloys. In section 5 we summarize our conclusion.

2. Itinerant ferromagnets

Magnetic valence, Z_m, is defined by eq. (5). $N_d^\uparrow$ is an integer, namely 0 or 5. Since to the right of Fe in the periodic table the spin-up (majority) d-band is filled, the values of Z_m are 2, 1, 0, −1, −2, ..., −7 for Fe, Co, Ni, Cu, Zn, ..., Br. Williams et al. [4] observed that in the late transition metals, the sp band contributes about 0.3 electrons to $N^\uparrow$ giving via eq. (5) Co and Ni the magnetic moments $\sim 1.6\,\mu_B$ and $\sim 0.6\,\mu_B$. By the same prescription one obtains for Fe a magnetic moment of $\sim 2.6\,\mu_B$. That the magnetic moment of Fe ($2.2\,\mu_B$) is in reality less than is due to its magnetic *weakness*. The examples of Fe, Co and Ni demonstrate that the magnetic moments obtained via

$$M = Z_m + 0.6 \tag{6}$$

serve as a zeroth-order guide. Deviations are either due to magnetic weakness or sp contributions to $N^\uparrow$ that differ from 0.3 [4].

The straight line defined by eq. (6) (together with experimental and calculated magnetic moments) is plotted in the left part of fig. 1. This is the generalized Slater–Pauling curve (GSP). We want to demonstrate that this curve is more than merely plotting the conventional Slater–Pauling (SP) curve by interchanging right and left. Consider e.g. the CoCr-alloy system. In the conventional SP curve the magnetic moments of CoCr alloys appear as a dramatic departure from regular behavior, whereas in fig. 1 the magnetic valence of $Z_m = -6$ for Cr and $Z_m = 1$ for Co places all values of the magnetic moments close to the left straight line. Fig. 1 shows, furthermore, that eq. (6) underestimates the magnetic moments of CoCr slightly. Thus, most likely, CoCr alloys are strong ferromagnets where Co and Cr form a

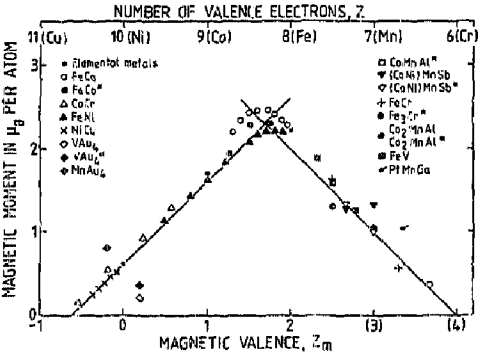

Fig. 1. Generalized Slater–Pauling curve. Magnetization per alloy atom versus magnetic valence Z_m in the left part, versus average number of valence electrons, Z, in the right part. Experimental data were taken from refs. 5–9. Calculated results (*) in ref. 10 for FeCo, refs. 11 and 15 for Heusler alloys, and this paper (VAu_4, CoMnSb, CoMnAl, Fe_3Cr).

common d band. Williams et al. [4] also showed that other departures from the conventional SP curve are removed, like NiV- and NiCr-alloys (not shown in fig. 1), which closely follow the GSP curve. It appears that with the exception of the strong ferromagnets FeCo [10] close to the vertex of fig. 1 all systems on the left are conventionally called *itinerant ferromagnets*.

We now turn to a rather exotic case. This is the magnetism of V in some compounds, like VPt_3 [12] and VAu_4 [8]. The case of VPt_3 is a difficult one which is deferred to another publication. VAu_4, however, poses no theoretical problems. Experimentally, it was found to be ferromagnetic with a moment per V ranging from 0.3 to 1 μ_B depending on the samples and investigators [8]. Thus the largest (and most recent) value for the magnetic moment *per atom* is $0.2\,\mu_B$. Where is this system to be placed on the GSP curve? If one allows that magnetic valence is not a fixed property of a given element but depends on the chemical environment, then one may assume in the case of VAu_4 (where the moment is presumably carried by V alone) that the magnetic valence of V is $Z_m = 5$. The coordinates of VAu_4 are now determined and its magnetic moment per atom can be included in

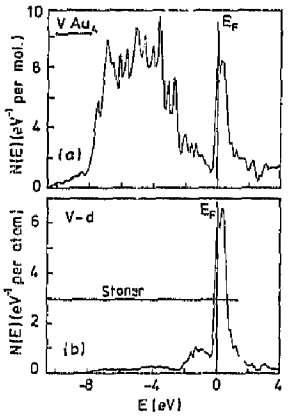

Fig. 2. Total density of states (DOS) of assumed non-magnetic VAu_4 (a) and partial d-DOS at V-site (b).

the GSP curve, see fig. 1. Using the ASW method [13] we have calculated the band structure of VAu_4 in the observed crystal structure [8]. Fig. 2 shows the total density of states (DOS) and that of d-character at the V-site of assumed non-magnetic VAu_4. The d-DOS of the V-site is reminiscent of that of V in VPd_3 [14] and its value at the Fermi energy well exceeds the critical (Stoner) value that is indicated in fig. 2b. Fig. 3 shows the DOS for ferromagnetic VAu_4 which possesses a calculated moment of 1.8 μ_B per V or 0.36 μ_B per atom. Fig. 3b reveals why VAu_4 appears as an exception in fig. 1: the Fermi energy cuts through the majority-spin d band; VAu_4 is an extremely weak itinerant ferromagnet. We close this section by mentioning the case of $MnAu_4$ [7, 8]. Assuming for the magnetic valence of Mn a value of 3, we can place it on the GSP curve and conclude from fig. 1 that $MnAu_4$ is a strong itinerant ferromagnet.

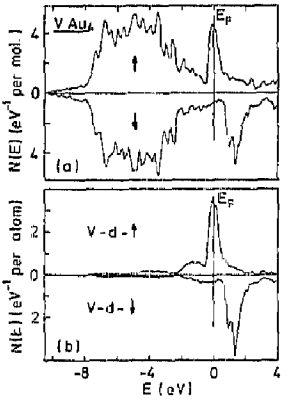

Fig. 3. Total majority-spin (↑) and minority-spin (↓) density of states (DOS) of ferromagnetic VAu_4 (a). Partial majority- and minority-spin d-DOS at V-site (b).

3. Localized moment systems

We now turn to the right part of fig. 1 which is defined by the straight line

$$M = Z - 6. \tag{7}$$

This constitutes the remainder of the GSP curve. Fig. 1 shows that the magnetic moments per atom of a large number of alloys (including Heusler alloys) are in zeroth order given by eq. (7). Most of these systems are considered to be ideal local moment systems [11].

Our estimate of the number of minority electrons per atom of $N^{\downarrow} = 3$ originates primarily from the band structure of Heusler alloys having the generic formula XMnY and $C1_b$ crystal structure. De Groot et al. [15] were the first who discovered their peculiar electronic structure: they found that in the case of NiMnSb and PtMnSb the majority-spin electrons are metallic, whereas the minority-spin electrons are semiconducting. They called these systems half-metallic ferromagnets. We want to review the essentials using as an example CoMnSb which we show here also to belong to the class of half-metallic ferromagnets. The crystal structure is shown in fig. 4b. Our self-consistent band structure of CoMnSb is shown in fig. 5a for the majority-spin electrons and in fig. 5b for the minority-spin electrons. The minority-spin electrons are obviously semiconducting, nine electrons fill exactly one s band, one p band, and one d band (no spin-degeneracy!). Thus we have $N^{\downarrow} = 3$ per atom and the calculated moment is exactly 1 μ_B

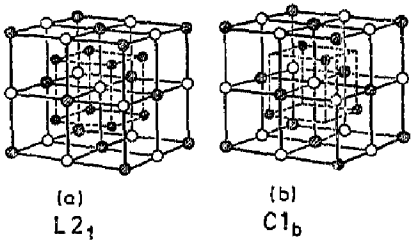

Fig. 4. $L2_1$ crystal structure (a), $C1_b$ (b) obtained by removing four black dots from (a). $C1_b$ is the crystal structure of CoMnSb, shaded circles Sb, white ones Mn, black ones Co.

per atom or 3 μ_B per molecule (calculated Mn moment is 3.2 μ_B), whereas the measured value is 4 μ_B per molecule [9]. It is worthwhile to stress at this point that our results are spin-moments whereas experimental values include orbital contributions (through a g-factor that may be different from 2).

Why are the minority-spin electrons semiconducting in the $C1_b$ but not in the $L2_1$ structure? To answer this question we show in fig. 6 the spin projected DOS for CoMnSb using this system as an example for the presently known half-metallic ferromagnets. The spin- and site projected d-DOS are shown in fig. 7. The latter (fig. 7b) shows that the peak structure of the spin-down Mn d electrons is tied to that of the spin-down d electrons of Co. Fig. 5b reveals that the peak 0.5 eV below E_F originates from t_{2g} electrons. Comparing in fig. 8 the DOS of the minority d electrons of Mn and Co with the DOS of the spin-down p electrons of Sb we see again a common peak 0.5 eV below E_F. De Groot [16] argues convincingly that this is the signature of a

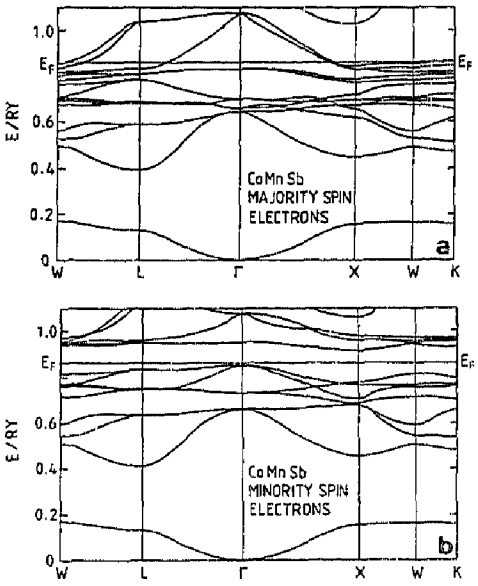

Fig. 5. (a) Band structure of majority-spin electrons; (b) of minority-spin electrons of CoMnSb.

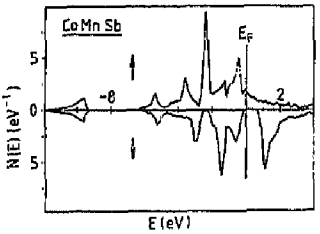

Fig. 6. Total majority-spin ↑ and minority-spin ↓ density of states of CoMnSb.

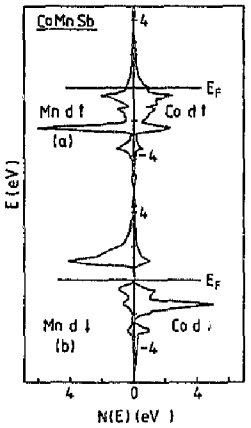

Fig. 7. Majority-spin d-density of state (DOS) of Mn and Co (a), minority d-DOS of Mn and Co (b).

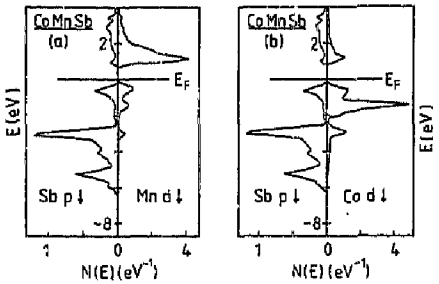

Fig. 8. Minority-spin p-density of state (DOS) for Sb compared with minority d-DOS of Mn (a) and of Co (b).

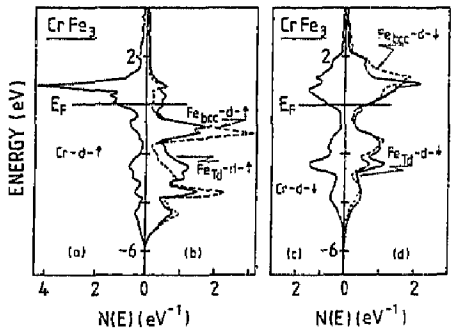

Fig. 9. $CrFe_3$ d-density of states (DOS), majority-spin d-DOS of Cr (a), and of Fe (b). There are two inequivalent Fe-sites, one surrounded by eight Fe atoms (labeled bcc), the other one by four Fe and four Cr atoms (labeled Td). Minority-spin d-DOS of Cr (d), and of Fe (d).

'Co induced Mn–Sb covalent interaction' which can be visualized by placing a p orbital on the Sb site and a t_{2g} orbital on each of the Co and Mn sites in fig. 4. If one attempts to align these orbitals in such a way that a bonding configuration results, one discovers that this is not possible in the $L2_1$ structure whereas the $C1_b$ structure allows such a configuration. Absence of the common peaks in the $L2_1$ structure (see ref. 11, fig. 18) supports this point of view. Bonding and antibonding states are thus tied to the strong exchange splitting of Mn via the t_{2g} states of Co (of Ni, Pt, or possibly even Ir in other cases). The Fermi energy lies midway between these states if the electron count of the bonding partner of Mn is correct. In the case of CoMnSb there are 4.5 spin-down Co electrons, 2 spin-down Mn electrons and 2.5 spin-down Sb electrons exactly filling the three bands. In the case of NiMnSb the moment per molecule is 4 μ_B [the average moment per atom follows eq. (7)!]; therefore, there are now 5 spin-down Ni electrons, 1.5 spin-down Mn electrons and 2.5 spin-down Sb electrons, again, filling exactly the three bands. Replacing Sb by Sn we find a band gap, but the Fermi energy now cuts through minority bonding states.

Returning to the generalized Slater–Pauling curve (fig. 1) we see that our zeroth-order estimate, eq. (7), is also valid for a class of binary alloys like FeV and FeCr. The reason is demonstrated for a representative case: $CrFe_3$, which has the $AlFe_3$ structure. Shown in fig. 9 are our results for the d state densities which are seen to form a common band where the Fermi energy (figs. 9c and d) is pinned in the central valley of the bcc-like minority-spin state densities. The same situation is found in pure bcc Fe and is expected to occur in FeV. The pinned Fermi energy fixes the number of minority-spin electrons $N^{\downarrow}$ close to 3 causing the magnetization to vary as Z.

4. Paramagnetic Curie temperatures

It is tempting to maintain that all alloy systems on the right part of the GSP curve constitute local-moment systems. This, however, can only be demonstrated for Heusler alloys having $L2_1$ crystal structure, which we have done elsewhere [11]. Similar arguments apply to Heusler alloys having $C1_b$ crystal structure for which we want to present new results here. Our strongest argument for considering the magnetic moments to be local is supplied by calculations which assume ferromagnetic and different antiferromagnetic moment alignments: the magnitudes of the magnetic moments changes by less than 5% in all cases. We thus are led to assume the validity

of the Heisenberg model. In particular, we calculate fully self-consistently the total energies, E_{tot}(ferro), for ferromagnetic, and E_{tot}(AFI) as well as E_{tot}(AFII), for two different antiferromagnetic moment alignments. The AFI alignment is characterized by alternating ferromagnetic planes parallel to the (001) plane, AFII by alternating ferromagnetic planes parallel to the (111) plane. For further details see ref. 11.

The total-energy differences

$$\Delta E_{\mathrm{I}} = E_{tot}(\text{ferro}) - E_{tot}(\text{AFI}),$$
$$\Delta E_{\mathrm{II}} = E_{tot}(\text{ferro}) - E_{tot}(\text{AFII}), \tag{8}$$

can then be used to determine two Heisenberg constants. This is possible, provided we require (1) that the total-energy differences are fully representable by the Heisenberg Hamiltonian, which, after a little algebra, leads to

$$\Delta E_{\mathrm{I}} = -4S^2 \sum_i z_i^{\mathrm{I}} J_i,$$
$$\Delta E_{\mathrm{II}} = -4S^2 \sum_i z_i^{\mathrm{II}} J_i, \tag{9}$$

where z_i^{I} and z_i^{II} give the coordination numbers for oppositely ordered moments, i.e. $z_i^{\mathrm{I}} = 8, 0, 16, \ldots$ and $z_i^{\mathrm{II}} = 6, 6, 12, \ldots$ for $i = 1, 2, 3, \ldots$, and (2) that it is possible to truncate the sums of eq. (9) including nearest and next-nearest neighbors only. In this case

$$\Delta E_{\mathrm{I}} = -32S^2 J_1,$$
$$\Delta E_{\mathrm{II}} = -24S^2(J_1 + J_2). \tag{10}$$

With the calculated total-energy differences, ΔE_{I} and ΔE_{II}, we then obtain J_1 and J_2 and from these the paramagnetic Curie temperature, θ, by means of the well-known formula

$$\theta = 4S(S+1)(2J_1 + J_2)/k_B. \tag{11}$$

Exchange constants from eq. (10) and paramagnetic Curie temperatures from eq. (11) are given in table I together with experimental values for three $L2_1$-Heusler alloys and three $C1_b$-Heusler alloys. Results for the latter are new. Table I shows that computed total-energy differences (which are zero temperature quantities) indeed allow fairly successful estimates of paramagnetic Curie temperatures.

Table I
Calculated exchange constants J_1 and J_2 and paramagnetic Curie temperatures, θ_{calc}, from eq. (11) ($L2_1$-Heusler alloys from ref. 11, $C1_b$-Heusler alloys this paper). $(T_c)_{exp}$ are measured Curie temperatures (from ref. 9)

		J_1 [meV]	J_2 [meV]	θ_{calc} [K]	$(T_c)_{exp}$ [K]
Co_2MnAl	($L2_1$)	0.840	0.062	808	697
Cu_2MnAl	($L2_1$)	0.333	0.329	690	630
Pd_2MnSn	($L2_1$)	0.178	−0.019	285	189
CoMnSb	($C1_b$)	0.431	0.120	600	490
NiMnSb	($C1_b$)	0.307	0.218	770	720
PtMnSb	($C1_b$)	0.281	0.139	650	575

5. Conclusion

We close our discussion by emphasizing the important role that band-structure calculations play in the present investigation. They are used, on the one hand, to throw light on systematic trends in a large amount of magnetization data. On the other hand, they can clarify the physics of unusual single cases like the interesting half-metallic ferromagnets [15]. Besides ground-state properties they can, at least in some cases, be successfully employed to calculate exchange constants and hence Curie temperatures. The crucial point here is to compare calculationally the ground states of magnetically ordered systems of different moment alignments. Comparing magnetic with non-magnetic ground states leads nowhere in this context.

Acknowledgement

The author has profitted from stimulating discussions with Dr. A. R. Williams regarding the Slater–Pauling curve and with Dr. R.A. de Groot concerning the half-metallic ferro-magnets. Part of this work was supported by Sonderforschungsbereich 65 Frankfurt-Darmstadt.

References

[1] Ch. Kittel, Introduction to Solid State Physics (Wiley, New York, 1968) p. 470.

[2] J. Friedel, Nuovo Cim. Suppl. No. 2 (1958) 287.
[3] K. Terakura and J. Kanamori, Prog. Theor. Phys. 46 (1971) 1007.
[4] A.R. Williams, V.L. Moruzzi, A.P. Malozemoff and K. Terakura, IEEE Trans. on Magn. MAG-19 (1983) 1983; see also: A.P. Malozemoff, A.R. Williams and V.L. Moruzzi, Phys. Rev. B29 (1984) 1620.
[5] R.M. Bozorth, Ferromagnetism (Van Nostrand, New York, 1951) p. 441.
[6] S. Chikazumi, Physics of Magnetism (Wiley, New York, 1964) p. 75.
[7] Landolt-Börnstein, Zahlenwerte und Funktionen, 6th ed., vol. II, part 9 (Springer, Berlin, 1962).
[8] K. Adachi, M. Matsui and Y. Fukuda, J. Phys. Soc. Jap. 48 (1980) 62.
[9] C.C.M. Campbell, J. Phys. F5 (1975) 1931.
[10] K. Schwarz, P. Mohn, P. Blaha and J. Kübler, J. Phys. F, submitted.
[11] J. Kübler, A.R. Williams and C.B. Sommers, Phys. Rev. B 28 (1983) 1745.
[12] R. Jesser, A. Bieber and R. Kuentzler, J. Phys. (Paris) 42 (1981) 1157.
[13] A.R. Williams, J. Kübler and C.D. Gelatt Jr., Phys. Rev. B 19 (1979) 6094.
[14] A.R. Williams, R. Zeller, V.L. Moruzzi, C.D. Gelatt, Jr. and J. Kübler, J. Appl. Phys. 52 (1981) 2067.
[15] R.A. de Groot, F.M. Mueller, P.C. van Engen and K.H.J. Buschow, Phys. Rev. Lett. 50 (1983) 2024.
[16] R.A. de Groot, private communication.